SLAC-PUB-1550
LBL-4227
March 1975

THE $\psi(3.1)$ AND THE SEARCH FOR OTHER NARROW RESONANCES OF SPEAR*

Presented by M. Breidenbach
Stanford Linear Accelerator Center
Stanford University, Stanford, California 94305

J. E. Augustin, A. M. Boyarski, F. Bulos, J. T. Dakin, G. J. Feldman, G. E. Fischer, D. Fryberger, G. Hanson, B. Jean-Marie, R. R. Larsen, V. Lüth, H. Lynch, D. Lyon, C. C. Morehouse, J. M. Paterson, M. L. Perl, B. Richter, B. Rapidis, R. F. Schwitters, W. Tanenbaum, F. Vannucci

Stanford Linear Accelerator Center
Stanford University, Stanford, California 94305

and

G. S. Abrams, D. Briggs, W. Chinowsky, C. E. Friedberg, G. Goldhaber, R. J. Hollebeek, J. A. Kadyk, A. Litke, B. Lulu, F. Pierre, B. Sadoulet, G. H. Trilling, J. S. Whitaker, J. Wiss, J. E. Zipse

Lawrence Berkeley Laboratory
University of California, Berkeley, California 94720

ABSTRACT

A sharp peak at 3.095 ± 0.005 GeV is seen in the cross section for e^+e^- annihilation. The width is $\Gamma = 77 \pm 19$ KeV. Angular distributions and interference effects imply that the J^{PC} of the $\psi(3.1)$ is 1^{--}. A study of the exclusive final states suggests that the G-Parity is odd. With the exception of another sharp resonance at 3.7 GeV, the $\psi(3.7)$, no other comparable structure is seen for masses between 3.2 and 5.9 GeV.

On observe un pic tres étroit a 3.095 ± 0.005 GeV dans la section efficace d'annihilation e^+e^-. La largeur est $\Gamma = 77 \pm 19$ KeV. Les distributions angulaires ainsi que les effets d'interference conduisent a assigner 1^{--} pour les nombres quantiques du $\psi(3.1)$. Une etude des canaux exclusifs suggère une parité G=-1. Si l'on exepte l'autre résonance $\psi(3.7)$, aucune structure comparable a eté trouvé entre 3.2 GeV et 5.9 GeV.

---

*Work supported by Energy Research and Development Administration

(Presented at the 9th Rencontre de Moriond, Meribel-les-Allues, France, March 8-14, 1975)

In November 1974, two narrow resonances coupled to e^+e^- at masses of 3.1 and 3.7 GeV were discovered.(1,2,3,4) A search(5) for other narrow resonances was conducted between 3.2 and 5.9 GeV, and no others of comparable strength were found. However, some interesting structure(6) in the total hadronic cross section from e^+e^- annihilation (σ_T) has been found near 4.1 GeV. This talk will attempt to describe the present experimental situation; it should be realized that many of the results are preliminary and therefore are not to be considered as firm or final.

The storage ring SPEAR circulates one bunch of electrons and one bunch of positrons in a single magnetic guide field. The bunches collide alternately in two interaction regions. The beam energies may now be varied between about 1.3 GeV and 4 GeV. The energy distribution of electrons within a beam bunch is approximately Gaussian with a width that increases approximately quadratically with energy, and has a σ of about 1 MeV at a total energy ($E_{cm} = 2\ E_{beam}$) of $E_{cm} = 3$ GeV. The absolute energy calibration is based on measurements of the particle orbits and the magnetic guide fields and is known to about 0.1% The bunch shapes are Gaussian with σ's in the transverse plane of approximately 0.1 cm and longitudinally a few cm. The luminosity is about $3 \times 10^{29}\ cm^{-2}\ sec^{-1}$ at $E_{cm} = 3$ GeV.

The magnetic detector is shown schematically in Fig. 1. The magnetic field of 4 kilogauss is axial and within a volume about 3 meters in diameter by 3 meters long. The interaction region is surrounded by a stainless steel vacuum pipe 0.15 mm thick. Coaxial with the pipe are a pair of cylindrical plastic scintillation counters that form one element of the trigger system. Continuing radially outward are four sets of multiwire spark chambers. Each set consists of four "planes" of wires at $\pm 2^o$ and $\pm 4^o$ with respect to the beam axis. Thus, each set of chambers provides redundant azimuthal (resolution ≈ 0.5 mm) and longitudinal (resolution ≈ 1.2 cm) position information for each charged particle. Following the spark chambers are a set of 48 plastic scintillator trigger counters. These counters are used in the trigger system and in a time-of-flight particle identification system with a resolution (σ) of about 0.5 nsec, allowing π/K separation up to about 0.6 GeV/c. Next comes the aluminum coil of the solenoid with a thickness of about 1 radiation length, followed by a layer of 24 lead-scintillator sandwich electron shower counters used to identify electrons. The next element is the iron return yoke of the magnet which also serves as a hadron filter for the final set of spark chambers which aid in muon identification.

The trigger requirement is two or more charged particles with transverse momenta greater than about 200 MeV/c. The complete detector system covers a solid angle of 0.65 x 4π. A hadronic event is defined to be one with 3 charged particles or two charged particles accolinear by 20° or more. The detector efficiency for hadronic events varies smoothly from 40% at E_{cm} = 2.5 GeV to 65% at 4.8 GeV. Backgrounds have been studied using separated beams and longitudinal (z) distributions of events. The background contribution to the resonances is very small, of order 0.01 to 0.1%, and is roughly 5% in the nonresonant region. Normally, cross sections are normalized by measuring Bhabha scattering in the magnetic detector. However, in the vicinity of the narrow resonances, the e^+e^- pair production cross section is strongly enhanced by photonic decays of the resonance. Hence, the luminosity is integrated by a set of small counters monitoring Bhabha scattering at small angles, (where the scattering is dominantly caused by space-like photons). The luminosity monitor is calibrated with the magnetic detector at a beam energy far from the resonances.

Figure 2 shows the total hadronic cross section versus E_{cm} in the region E_{cm} = 3.1 GeV. A sharp peak is seen at a mass of 3.095 $\pm$ 0.005 GeV. The peak cross section is rather large, approximately 2500 nb, and the observed width is about 2.5 MeV FWHM. The width is that expected from the convolution of a much narrower resonance shape, the inherent spectral resolution of the storage ring, and radiative corrections in the production of a virtual photon.

Figure 3a shows the cross section for production e^+e^- pairs; Figure 3b shows the cross section for $\mu^+\mu^-$ pairs. These data allow the determination of the total resonance width Γ and the width into electrons Γ_e and muons Γ_μ. The resonant cross section to any set of states f may be written

$$\sigma_f = \frac{(2J + 1)\pi}{W^2} \frac{\Gamma_e \Gamma_f}{(M-W)^2 + \Gamma^2/4}$$

where J is the spin of the resonance, W is the center-of-mass energy, M is the resonance mass, and Γ_f is the width to the set of final states. If this expression is integrated, it may be compared to the integrated experimental cross section (after appropriate radiative corrections) without explicit dependence on the storage ring energy resolution. Thus:

$$\int \sigma_f(W)\, dw = \frac{(2J + 1)\, 2\pi^2}{M^2} \frac{\Gamma_e \Gamma_f}{\Gamma} .$$

The integrated total hadronic cross section is $\int \sigma_h\, dw = 10.8 \pm 2.7$ nb GeV. Assuming that $\Gamma = \Gamma_h + \Gamma_\mu + \Gamma_e$ and that $\Gamma_\mu = \Gamma_e$ and that $J = 1$, $\Gamma = 77 \pm 19$ KeV and $\Gamma_e = 5.2 \pm 1.3$ KeV. The quoted errors are derived from the statistical errors combined in quadrature with the known systematic uncertainties, including hadron detection efficiency (10%), luminosity measurements (10%), and reproducability of the integral of the measured cross section (8%).

The analysis assumed $\Gamma_e = \Gamma_\mu$ (muon-electron universality) because the e-pair cross section has a large contribution from space-like momentum transfer QED processes. If the QED contributions are removed, then the ratio of the resonant μ to e cross sections is 0.99 ± 0.06. See Figures 4a and 4b.

The assumption that J=1 can be tested by examining the angular distribution of the produced μ's and e's. Figure 4a shows the angular distribution of the positron for e^+e^- production. The solid points are the measured data and the open points have the QED space-like contribution removed. Figure 4b shows the similar distribution for μ's. Both curves are for data in a E_{cm} interval of 1 MeV centered at the peak of the $\psi(3.1)$. A fit to the form $a + b \cos^2\theta$ yields a b/a ratio of 1.3 ± 0.2, thus suggesting that J=1. The expected value for J=1 is unity. The measured μ asymmetry at the resonance peak (forward μ^+ - backward μ^+ divided by total) is 0.014 $\pm$ 0.02, implying that either vector <u>or</u> axial vector accounts for at least 97% of the total resonant amplitude (95% confidence).

The parity of the $\psi(3.1)$ may be determined by looking for an interference between the resonant and QED amplitudes in the $\mu^+\mu^-$ channel. This interference is manifested in the energy dependence of the $\mu^+\mu^-$ cross section which is integrated over an angular interval centered at 90°. The resonant 1^- amplitude will interfere with the QED contribution destructively below the peak and constructively above. A resonant 1^+ amplitude will not interfere. Figure 5 shows the prediction for the ratio $\sigma_{\mu\mu}$ to σ_{ee} as a function of energy with and without interference (corresponding to 1^- and 1^+ amplitudes). The effect above the peak is obscured by the radiative corrections. This choice of the $\sigma_{\mu\mu}$ to σ_{ee} ratio is made to minimize systematic errors. Figure 6 shows the data. For the 1^- hypothesis, the interference dip extends from about 14 to 4 MeV below the peak. In a 4 MeV interval in this region, 1360 $e^{\pm}$ pairs were observed; we expect 100 $\pm$ 10 $\mu^{\pm}$ for no interference and 71 $\pm$ 8 with interference. We observe 68 $\mu^{\pm}$ which is over 3 standard deviations from the prediction for no interference and quite compatible with the interference hypothesis. We believe that the $\psi(3.1)$ has the same quantum numbers, J^{PC}, as the photon.

Several exclusive decay modes of the $\psi(3.1)$ have been identified. One of the interesting questions is the determination of the G-Parity and isospin of the $\psi(3.1)$ from its multipion decay states. It is possible to calculate the missing mass distribution according to the hypothesis $n(\pi^+\pi^-) + X$. Mass squared distributions for the X for n=2 and n=3 are shown in Figs. 7 and 8. A large peak near a mass square of 0 is seen. The resolution is inadequate to distinguish a π^0 from a single photon. The cross section in the peak for the $2(\pi^+\pi^-) + X$ is about 90 nb, the $3(\pi^+\pi^-) + X$ channel is about 60 nb, and the $\pi^+\pi^-$ X channel is somewhat smaller. A hint that the X is indeed a π^0 is shown in Figure 9. Here the sample of presumed $\pi^+\pi^-\pi^+\pi^-\pi^0$ events are binned in invariant mass intervals of the $\pi^+\pi^-\pi^0$ combination. A clean signal is seen at the mass of the ω.

Four constraint fits (measurement of all the particles of an event) have also been done. Figure 10 shows the total energy distribution of an event assuming a particle identification $\pi^+\pi^-\pi^+\pi^-$. The peak around 3.1 GeV indeed corresponds to this hypothesis. The peak at about 2.7 corresponds to $\pi^+\pi^-K^+K^-$, i.e., these events move to 3.1 GeV when appropriate particles are assigned kaon masses. States of $p\bar{p}$ and $\Lambda\bar{\Lambda}$ have been seen. The 4-C multipion status have a cross section consistent with that expected from the photonic decay of the $\psi(3.1)$ rather than a direct hadronic decay. If we take the $\psi(3.1) \rightarrow \mu^+\mu^-$ decay as a measure of the branching ratio for the ψ to decay via a virtual photon, we expect the cross section for any given exclusive final state to be enhanced by a factor of about 20 compared to its value just off resonance. The cross section for 2 $(\pi^+\pi^-)$ has been measured to be about 0.6 nb at W = 3.0 GeV; an enhancement by a factor of approximately 20 is observed. Conversely, an upper limit for the $2(\pi^+\pi^-) + \pi^0$ cross section off resonance is 0.6 nb; the observed resonant cross section is at least 150 times greater. The favored direct hadronic decay into states of odd numbers of π's would imply negative G-Parity and even isospin, probably 0.

Shortly after the discovery of the $\psi(3.1)$, SPEAR and the detector were modified to allow a sequential sweep in energy in steps of 1.8 MeV in E_{cm}. Measurements were made at each energy for several minutes, so that the expected hadron rate was about 2 per step. Realtime computation allowed an evaluation of the cross section within a few seconds of completion of an energy step. Using this technique, another narrow resonance was found at 3.7 GeV, and is named $\psi(3.7)$. After the discovery of the $\psi(3.7)$, the scanning process was continued up to a W of 5.9 GeV. The results are shon in Fig. 11. Only the $\psi(3.7)$ stands out clearly. The region below 3.2 GeV has not yet been finished. Upper limits on the resonance strength $\int\sigma_h dw$ for other narrow resonances are shown for various energy intervals in Table I. We hope to extend the range of the scan by a few GeV in the near future.

REFERENCES AND FOOTNOTES

1. J. J. Aubert et al., Phys. Rev. Letters 33, 1404 (1974).

2. J. E. Augustin et al., Phys. Rev. Letters 33, 1406 (1974).

3. C. Bacci et al., Phys. Rev. Letters 33, 1408 (1974).

4. G. S. Abrams et al., Phys. Rev. Letters 33, 1453 (1974).

5. A. M. Boyarski et al., "Search for Narrow Resonances in e^+e^- Annihilation in the Mass Region 3.2 to 5.9 GeV," submitted to Phys. Rev. Letters.

6. J. E. Augustin et al., "Total Cross Section for Hadron Production by e^+e^- Annihilation," submitted to Phys. Rev. Letters.

FIGURE CAPTIONS

1. (a) Telescoped view of detector; (b) end view of detector.

2. Total cross section for hadron production vs. center-of-mass energy for $\psi(3.1)$, corrected for detector acceptance.

3. Cross section for production of lepton pairs integrated over the range $|\cos\theta| \leq 0.6$ vs. center-of-mass energy; (a) electrons, (b) muons. No correction has been applied for the loss of events having $|\cos\theta| > 0.6$.

4. Angular distribution of the positive particle for production of lepton pairs. The center-of-mass energy is within 1 MeV of the peak of the $\psi(3.1)$. (a) Electrons. The solid points are measured; the open points have the QED contribution removed. (b) Muons. The curves are the expected distribution for a spin 1 resonance.

5. Predictions for the ratio of μ-yield to e-yield for no interference and complete interference.

6. Experimental data for the ratio of μ-yield to e-yield. The hypothesis of no interference can be excluded by having a confidence level of less than 0.15%.

7. Missing mass squared distribution for the hypothesis $\psi(3.1) \rightarrow \pi^+\pi^-\pi^+\pi^- + X$.

8. Missing mass squared distribution for the hypothesis $\psi(3.1) \rightarrow \pi^+\pi^-\pi^+\pi^-\pi^+\pi^- + X$.

9. Mass distribution of the $\pi^+\pi^-\pi^0$ combination in the decays $\psi(3.1) \rightarrow \pi^+\pi^-\pi^+\pi^-\pi^0$.

10. Total energy distribution for 4-constraint fits to 4 charged particles assuming all are π's. The peak at 3.1 corresponds to this hypothesis, and the lower energy peak corresponds to $\pi^+\pi^-K^+K^-$ production.

11. Relative cross sections from the fine mesh energy scan. The $\psi(3.7)$ is clearly visible.

TABLE I

Upper limits at the 90% confidence level for the radiatively corrected integrated cross section of a possible resonance. The units are nb Mev.

Mass range (GeV)	Resonance width (FWHM in MeV) 0[a]	10	20
3.200 to 3.500	970	1750	2230
3.500 to 3.690	780	1090	1540
3.720 to 4.000	1470	1530	1860
4.000 to 4.400	620	1260	1860
4.400 to 4.900	580	1080	1310
4.900 to 5.400	780	1100	1720
5.400 to 5.900	800	1120	1470

[a]Width less than the mass resolution

(a)

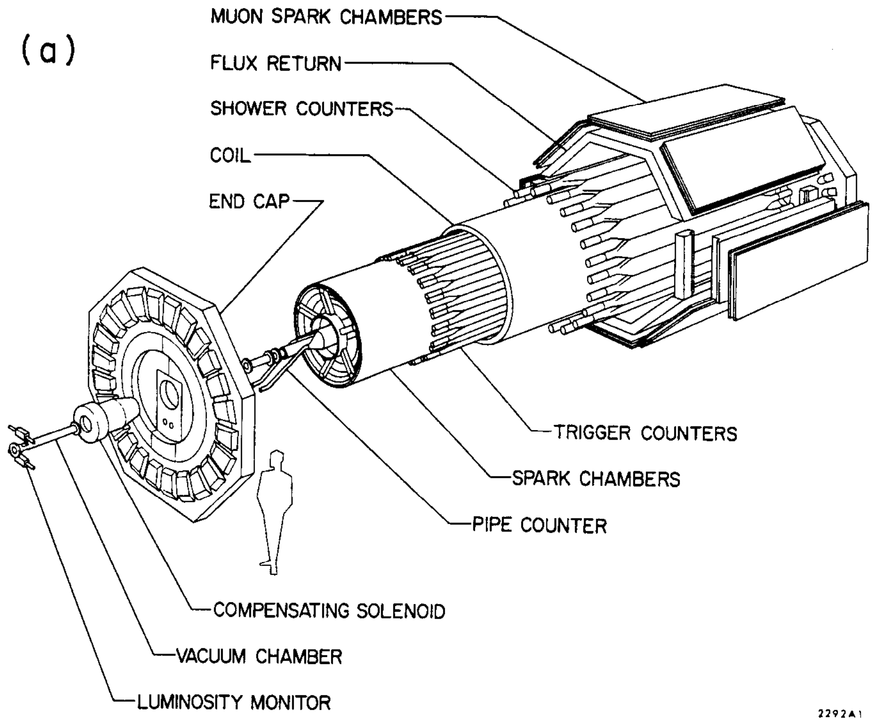

MUON SPARK CHAMBERS
FLUX RETURN
SHOWER COUNTERS
COIL
END CAP
TRIGGER COUNTERS
SPARK CHAMBERS
PIPE COUNTER
COMPENSATING SOLENOID
VACUUM CHAMBER
LUMINOSITY MONITOR
2292A1

(b)

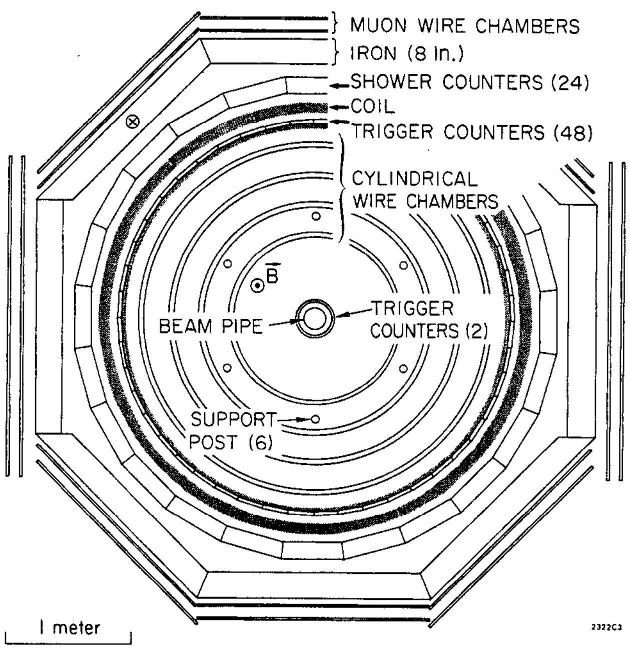

MUON WIRE CHAMBERS
IRON (8 in.)
SHOWER COUNTERS (24)
COIL
TRIGGER COUNTERS (48)
CYLINDRICAL
WIRE CHAMBERS
B
BEAM PIPE
TRIGGER
COUNTERS (2)
SUPPORT
POST (6)
1 meter

Fig. 1

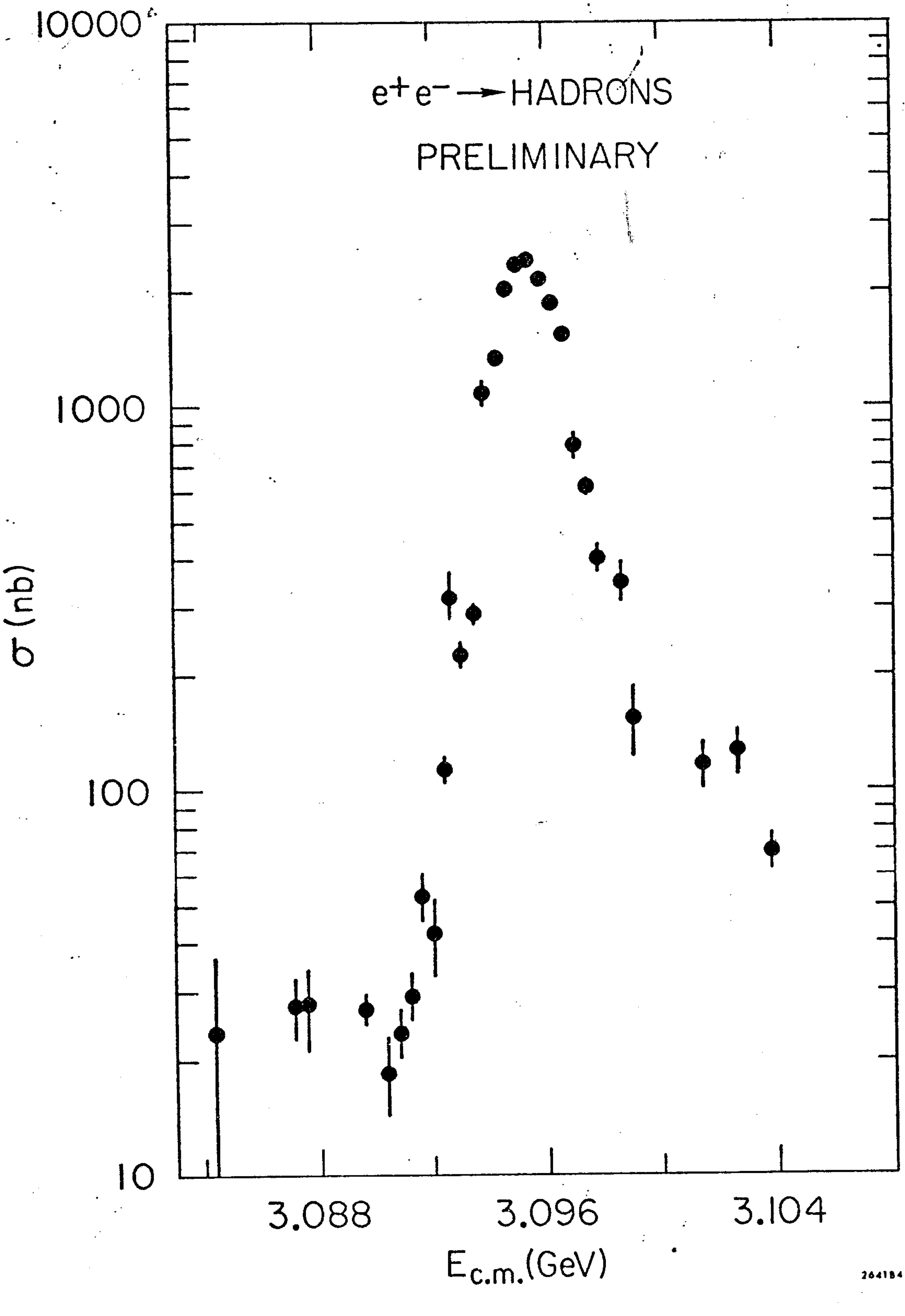
e+ e− → HADRONS
PRELIMINARY
10000
1000
100
10
σ (nb)
3.088
3.096
3.104
Ec.m.(GeV)
264184

Fig. 2

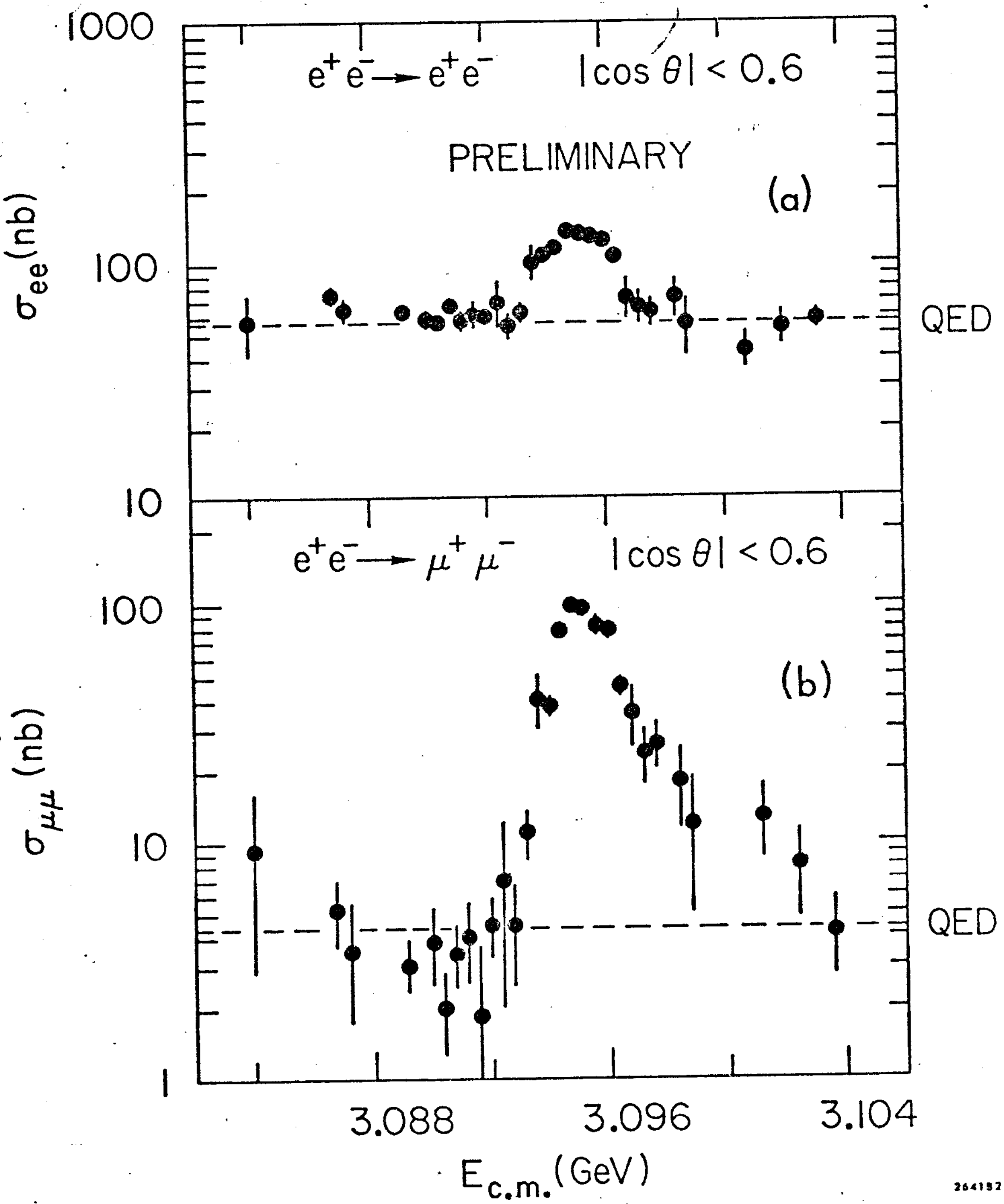
$e^+e^- \to e^+e^-$
$|\cos\theta| < 0.6$
PRELIMINARY
(a)
σ_{ee} (nb)
1000
100
10
QED
$e^+e^- \to \mu^+\mu^-$
$|\cos\theta| < 0.6$
(b)
$\sigma_{\mu\mu}$ (nb)
100
10
1
QED
3.088
3.096
3.104
$E_{c.m.}$ (GeV)
264152

Fig. 3

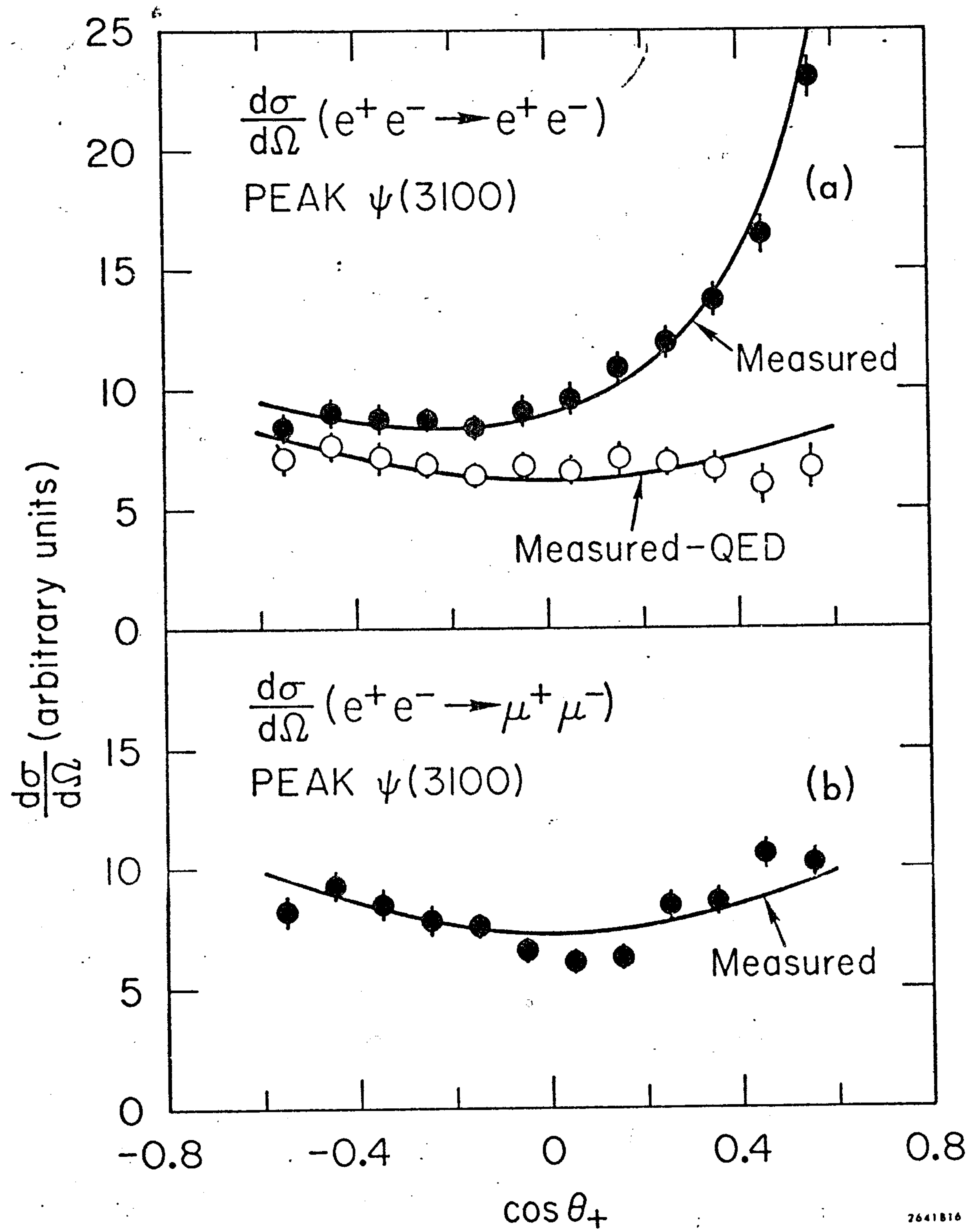

$\frac{d\sigma}{d\Omega}(e^+e^- \rightarrow e^+e^-)$
PEAK $\psi(3100)$
(a)
Measured
Measured-QED
$\frac{d\sigma}{d\Omega}(e^+e^- \rightarrow \mu^+\mu^-)$
PEAK $\psi(3100)$
(b)
Measured
$\frac{d\sigma}{d\Omega}$ (arbitrary units)
$\cos\theta_+$
2641B16

Fig. 4

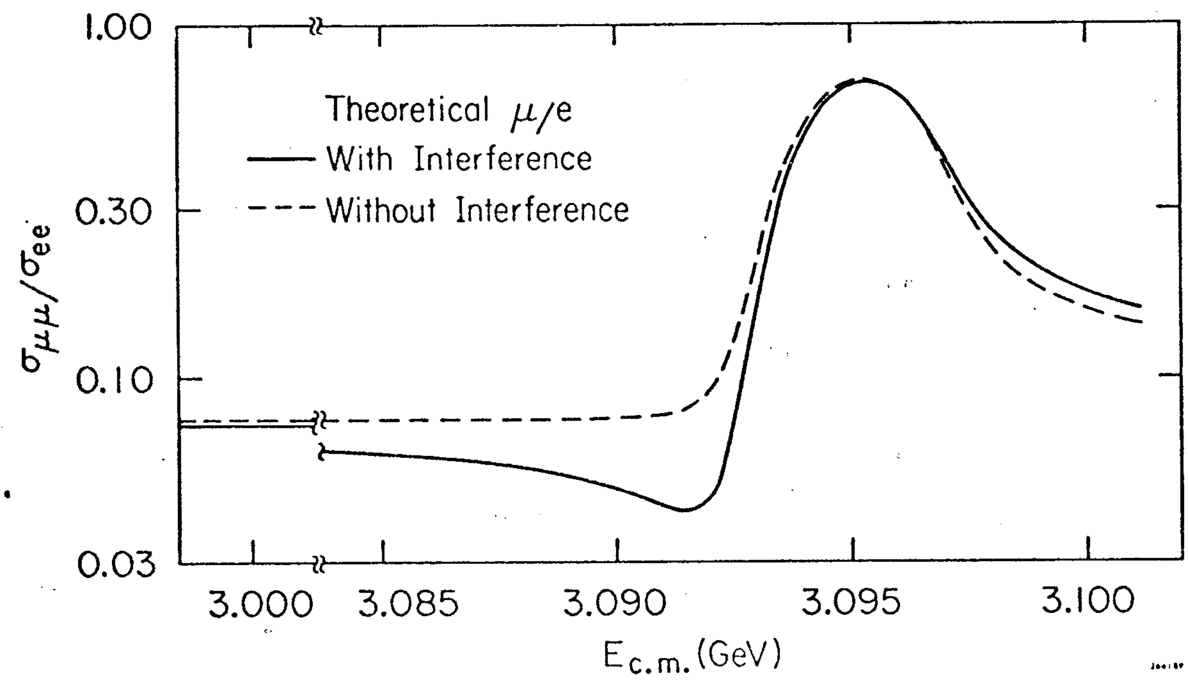
1.00
0.30
0.10
0.03
$\sigma_{\mu\mu}/\sigma_{ee}$
Theoretical μ/e
With Interference
Without Interference
3.000
3.085
3.090
3.095
3.100
$E_{c.m.}$ (GeV)

Fig. 5

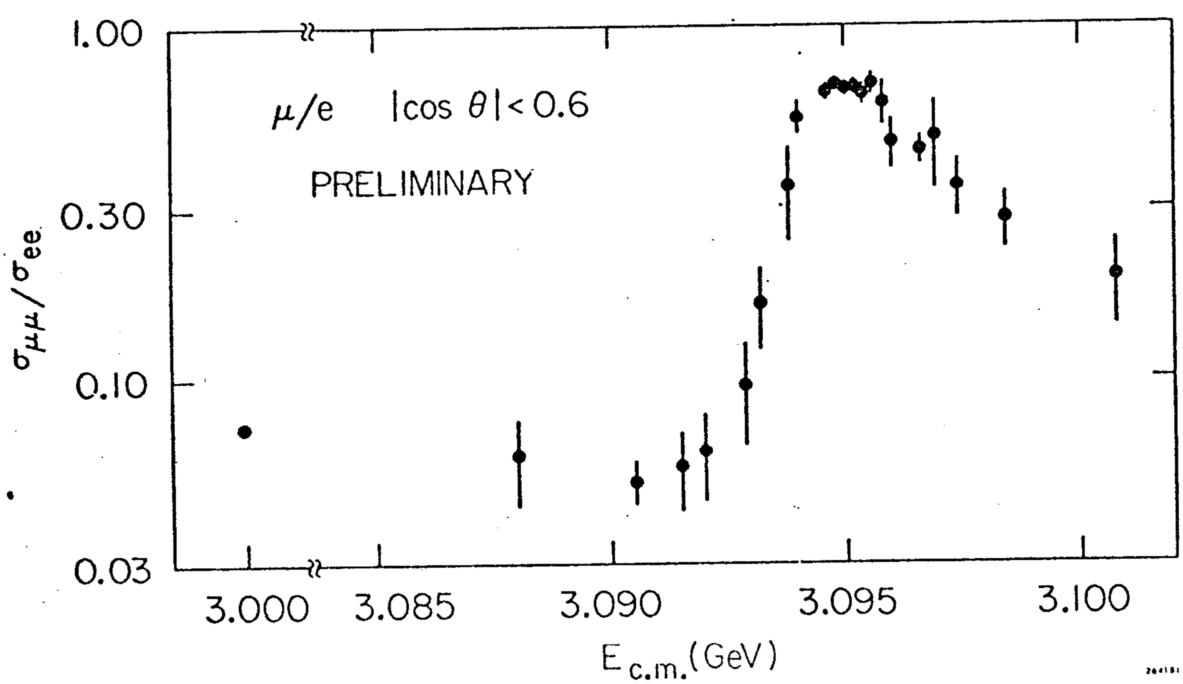
1.00
0.30
0.10
0.03
$\sigma_{\mu\mu}/\sigma_{ee}$
μ/e $|\cos\theta| < 0.6$
PRELIMINARY
3.000
3.085
3.090
3.095
3.100
$E_{c.m.}$ (GeV)

Fig. 6

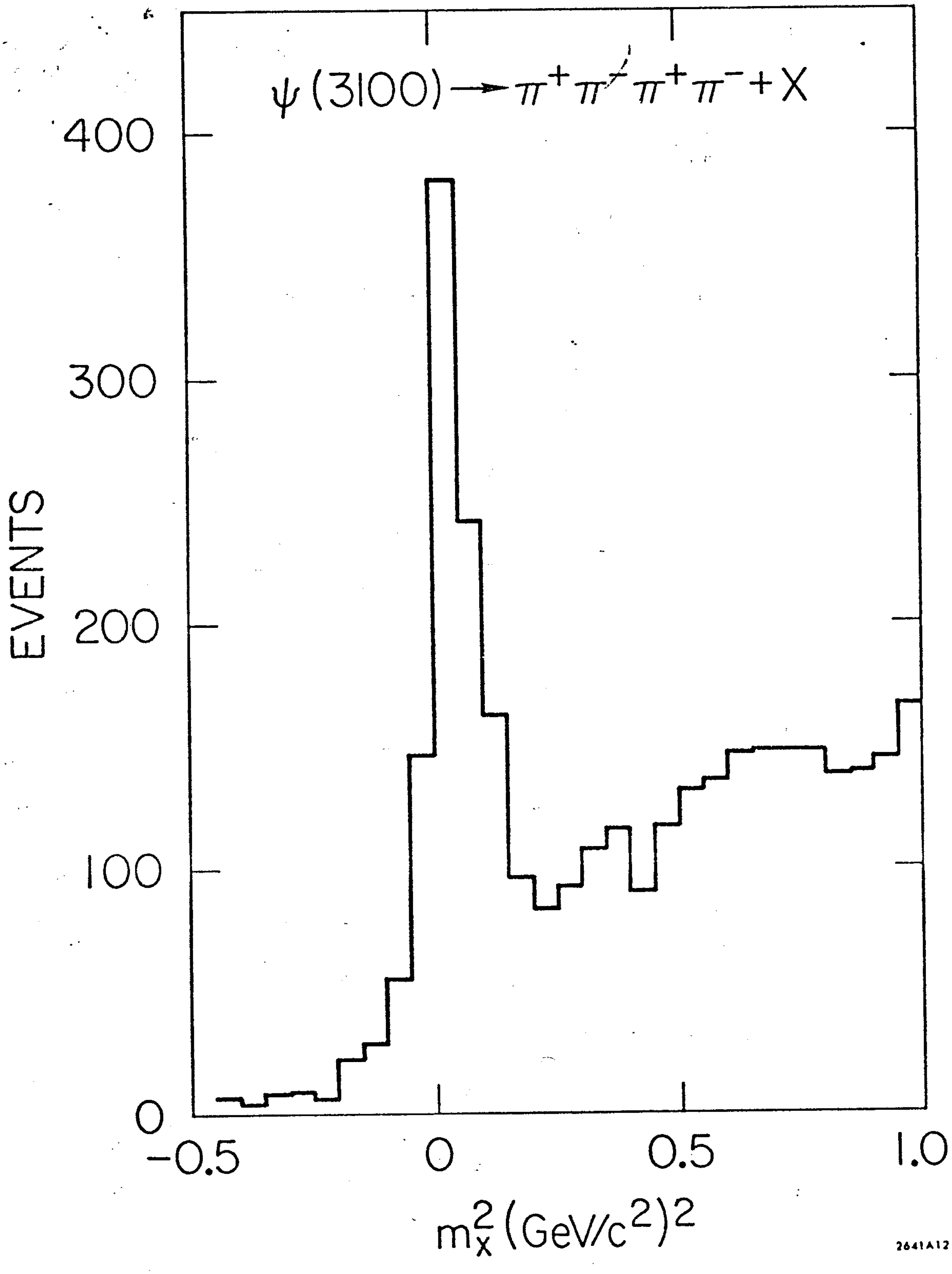

$\psi(3100) \rightarrow \pi^+\pi^-\pi^+\pi^- + X$
400
300
200
100
0
EVENTS
−0.5
0
0.5
1.0
$m_X^2\ (\mathrm{GeV}/c^2)^2$
2641A12

Fig. 7

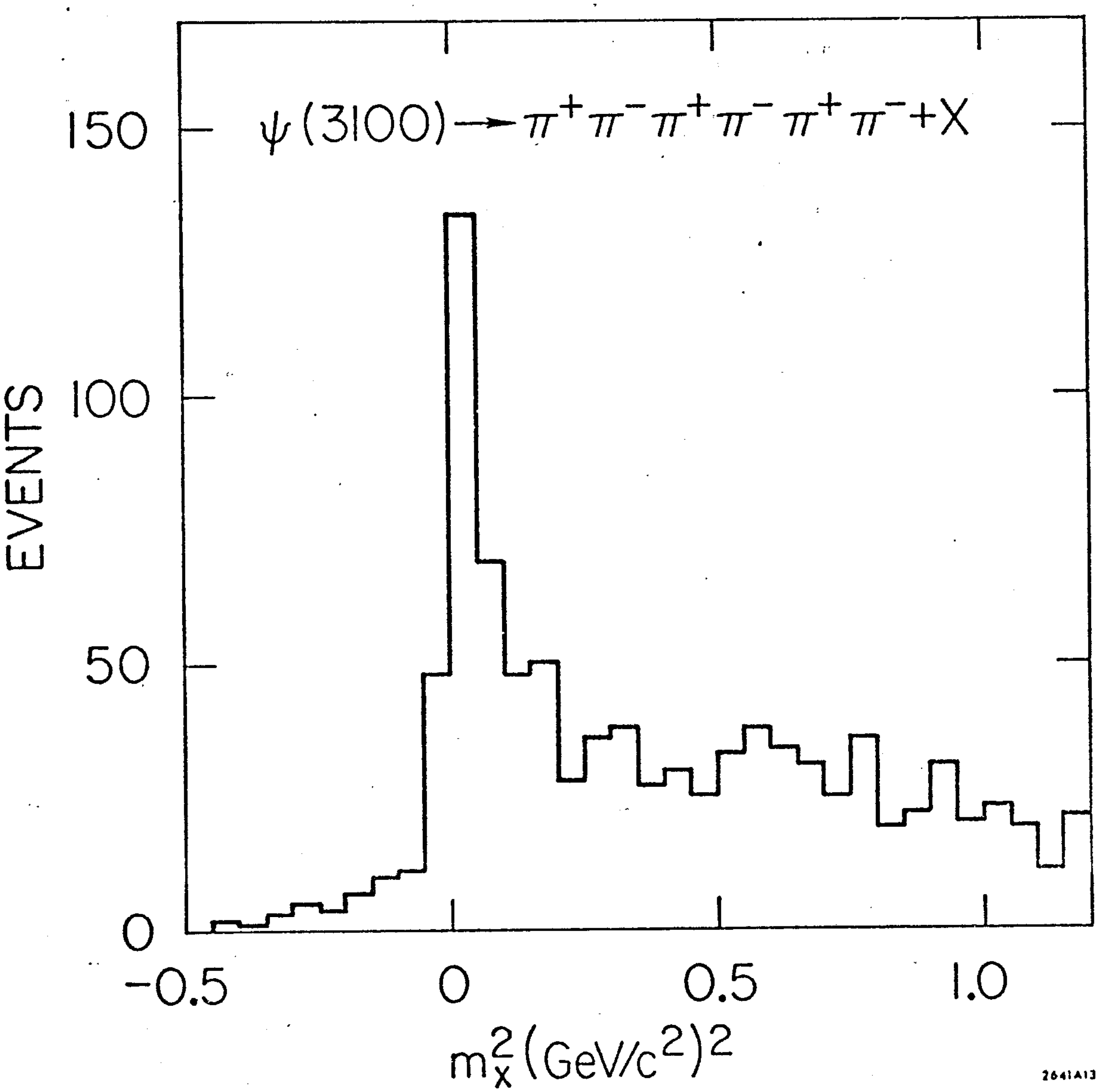

$\psi(3100) \rightarrow \pi^+\pi^-\pi^+\pi^-\pi^+\pi^- + X$
150
100
50
0
EVENTS
−0.5
0
0.5
1.0
$m_X^2\,(\mathrm{GeV}/c^2)^2$
2641A13

Fig. 8

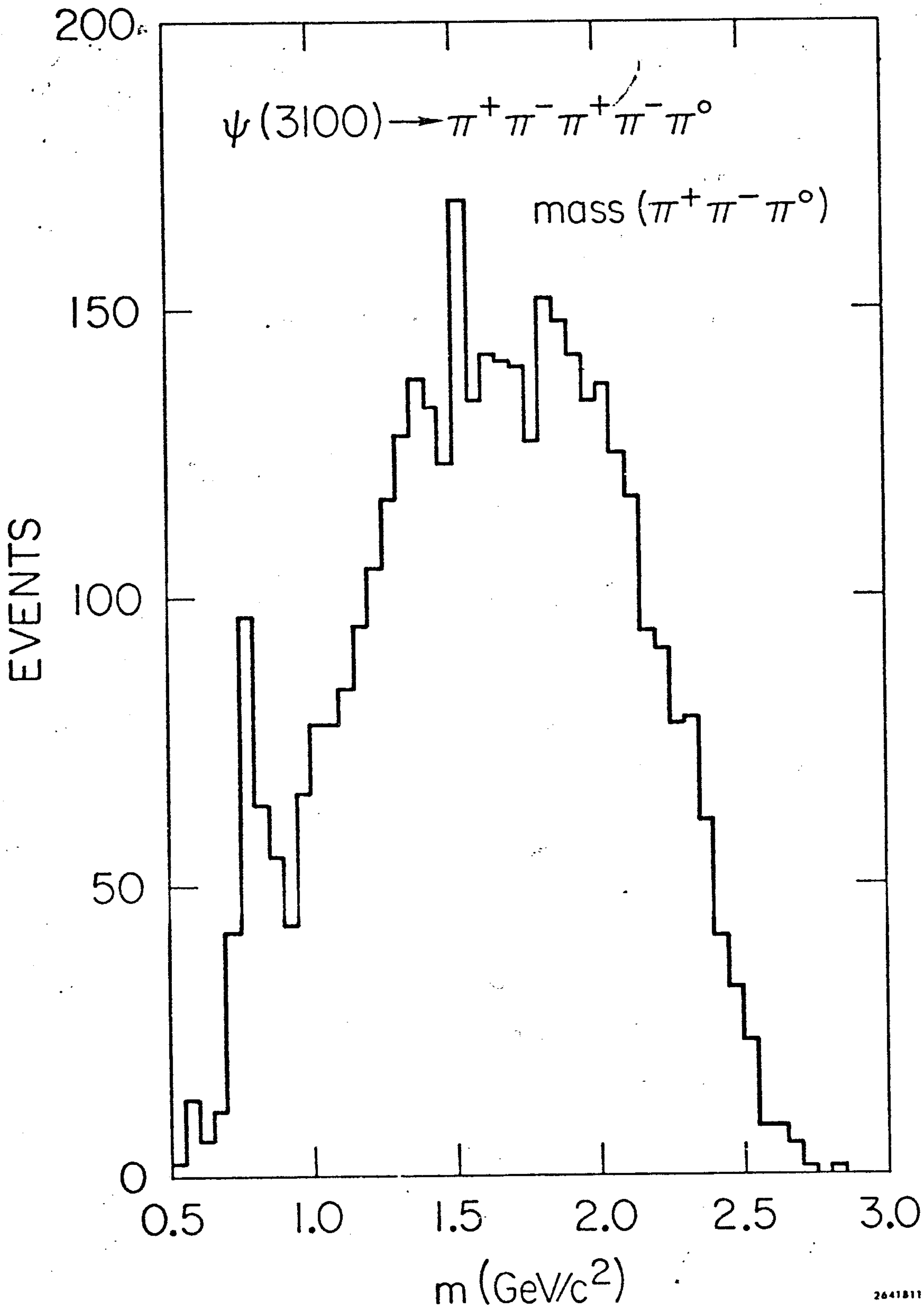

$\psi(3100) \rightarrow \pi^+\pi^-\pi^+\pi^-\pi^\circ$
mass $(\pi^+\pi^-\pi^\circ)$
EVENTS
200
150
100
50
0
0.5
1.0
1.5
2.0
2.5
3.0
m (GeV/c^2)
2641B11

Fig. 9

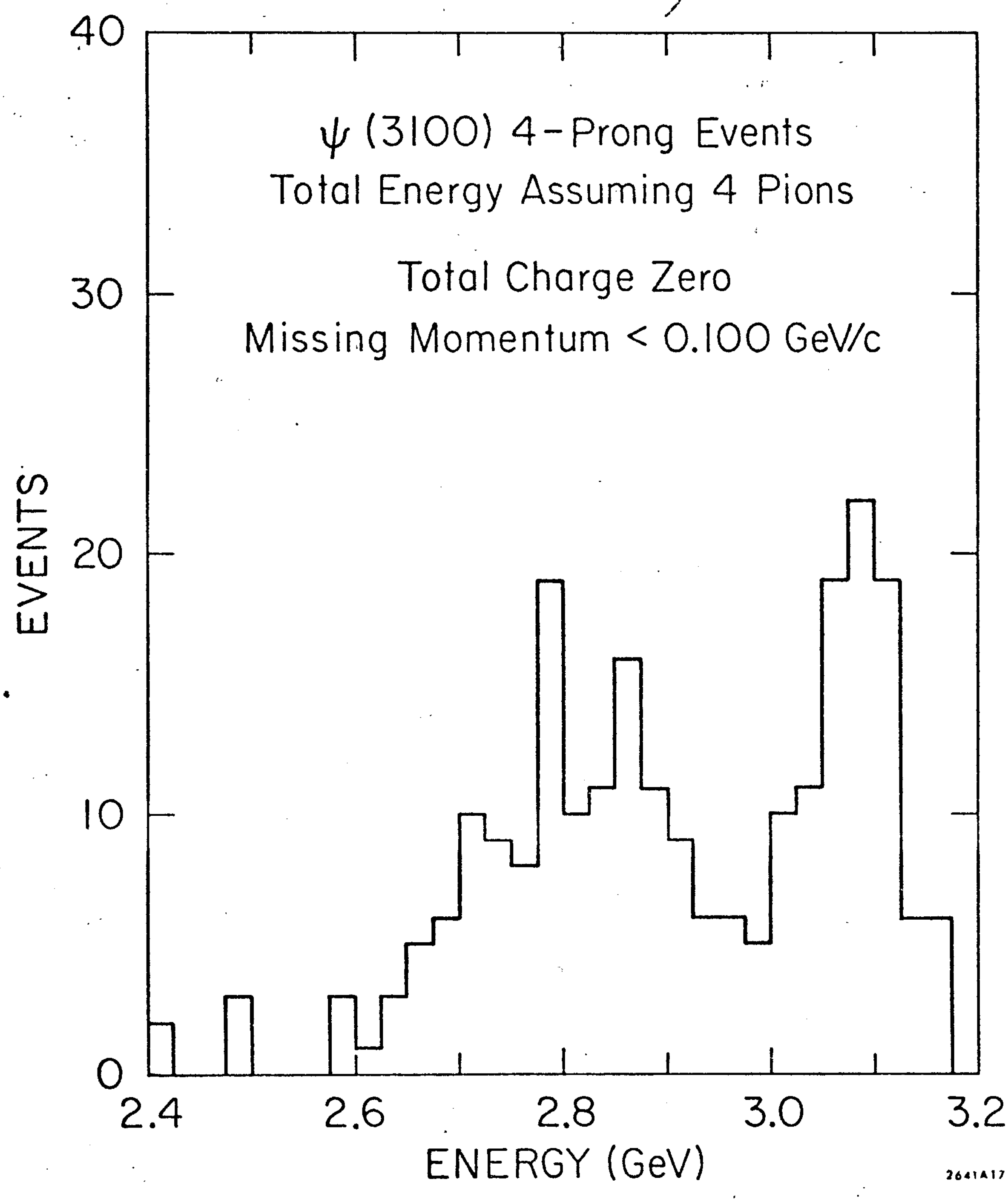

ψ (3100) 4-Prong Events
Total Energy Assuming 4 Pions
Total Charge Zero
Missing Momentum < 0.100 GeV/c
EVENTS
40
30
20
10
0
2.4
2.6
2.8
3.0
3.2
ENERGY (GeV)
2641A17

Fig. 10

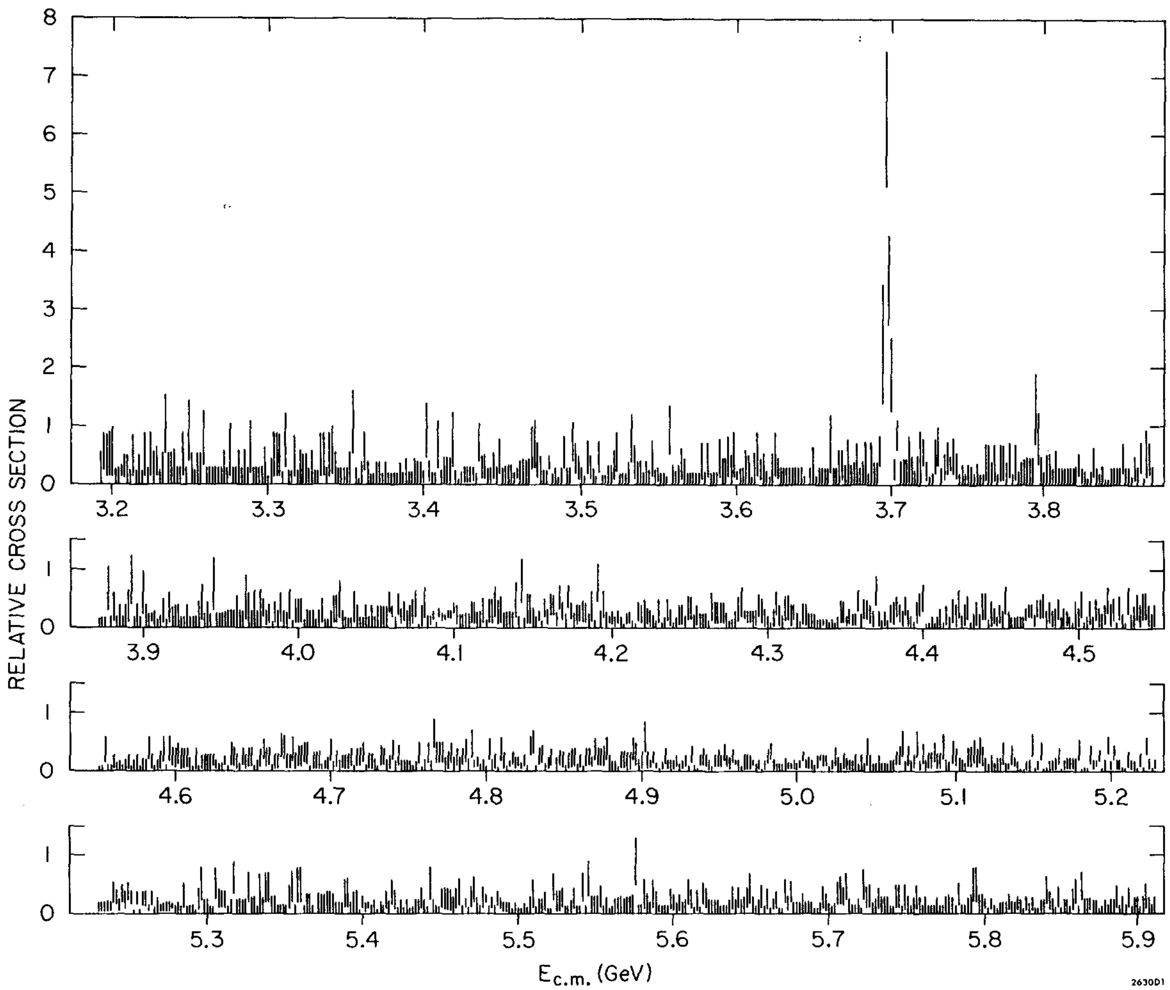

Fig. 11